Journal of Applied Polymer Science

Poly(ethylene glycol) methyl ether methacrylate-*graft*-chitosan nanoparticles as a biobased nanofiller for a poly(lactic acid) blend: Radiation-induced grafting and performance studies

Parichart Kongkaoroptham,[1,2] Thananchai Piroonpan,[2] Kasinee Hemvichian,[3] Phiriyatorn Suwanmala,[3] Watcharee Rattanasakulthong,[4] Wanvimol Pasanphan[1,2]

[1]Department of Materials Science, Faculty of Science, Kasetsart University, 50 Ngam Wong Wan Road, Ladyao, Chatuchak, Bangkok 10900, Thailand

[2]Center of Radiation Processing for Polymer Modification and Nanotechnology (CRPN), Department of Materials Science, Faculty of Science, Kasetsart University, 50 Ngam Wong Wan Road, Ladyao, Chatuchak, Bangkok 10900, Thailand

[3]Thailand Institute of Nuclear Technology, Ministry of Science and Technology, Saimoon, Onkharak, Nakhon-Nayok 26120, Thailand

[4]Department of Physics, Faculty of Science, Kasetsart University, 50 Ngam Wong Wan Road, Ladyao, Chatuchak, Bangkok 10900, Thailand

Correspondence to: W. Pasanphan (E-mail: wanvimol.p@ku.ac.th)

ABSTRACT: In this study, we aimed to modify chitosan (CS) as a novel compatible bio-based nanofiller for improving the compatibility including the thermal and mechanical properties of poly(lactic acid) (PLA). The modification of CS with poly(ethylene glycol) methyl ether methacrylate (PEGMA) was done by radiation-induced graft copolymerization. The effects of the dose rate, irradiation dose, and PEGMA concentration on the degree of grating (DG) were investigated. The chemical structure, packing structure, thermal stability, particle morphology, and size of the PEGMA-*graft*-chitosan nanoparticles (PEGMA-*graft*-CSNPs) were characterized by fourier transform infrared spectroscopy, X-ray diffraction, thermogravimetric analysis, and transmission electron microscopy. The compatibility of the PEGMA-*graft*-CSNP/PLA blends was also assessed by field emission scanning electron microscopy. The PEGMA-*graft*-CSNPs exhibited a spherical shape with the DG and particle sizes in the ranges of 3–145% and 35–104 nm, respectively. The PEGMA-*graft*-CSNPs showed compatible with PLA because of the grafted PEGMA segment. A model case study of the PEGMA-*graft*-CSNP/PLA blend demonstrated the improvement not only the compatibility but also thermal stability flexibility, and ductility of PLA. © 2015 Wiley Periodicals, Inc. J. Appl. Polym. Sci. **2015**, *132*, 42522.

KEYWORDS: bio-based nanofiller; chitosan nanoparticle; compatibility; poly(lactic acid); radiation grafting

Received 24 January 2015; accepted 19 May 2015
DOI: 10.1002/app.42522

INTRODUCTION

Poly(lactic acid) (PLA), an aliphatic polyester and hydrophobic polymer, is one of the most popular biodegradable plastics for replacing petroleum-based polymers in the recent year. It is produced by polymerization of lactic acid or lactide, which is produced by a fermentation of agriculture residue materials (e.g., corn or cassava).[1] PLA exhibits biodegradability, biocompatibility, nontoxicity, and good mechanical properties comparable to the commodity polymers.[2] Therefore, it has been received much attention for the development of various end-use applications, such as packaging materials.[3] However, its brittleness and nonstability at high temperatures restrict its capability for such purposes.

The modification of PLA by the addition of plasticizers, nonbiodegradable, and biodegradable fillers is a well-known procedure for improving the PLA properties.[4] Cellulose ester,[5] citric acid,[6] glycidyl methacrylate,[7] and poly(ethylene glycol) (PEG)[8] are widely used plasticizers for PLA. For example, PLA containing PEG plasticizer exhibited greater enzymatic degradation than neat PLA.[8] As PEG is a low-molecular-weight material, it can be well compatible with the PLA matrix; this leads to improvements in the elongation at break, ductility, processability, and flexural properties.[9] PEG and its derivatives are nontoxic, biocompatible, biodegradable, and food-contactable plasticizers for PLA blends.[10–14] However, the small-molecular-weight plasticizers easily migrate from the bulk polymer to the surface, and this results in changes in the mechanical

properties.[15] For nonbiodegradable polymers, they significantly enhance the mechanical and thermal properties of PLA. However, their nonbiodegradable nature obstructs the inherent biodegradable efficiency of PLA. Several types of nonbiodegradable polymers, for example, polypropylene[16] and polyurethane,[17] have been blended with PLA. One of the reasonable approaches for improving the PLA properties is its blending with biodegradable polymers, particularly from renewable resources, such as starch,[18] natural wood,[19] cellulose fibers,[20] and chitosan (CS).[21] In this way, various desirable properties of PLA can be improved without any hindrance in their inherent biodegradable properties.[4]

CS, a naturally occurring biopolymer, has been investigated for PLA blends. CS exhibits biodegradable, biocompatible, edible, antimicrobial, oxygen-impermeable, and nontoxic properties. These properties are of great interest for development as biobased fillers in PLA, particularly for food-packaging materials. For example, Wan *et al.*[22] reported that CS could improve the wettability when it was blended with biodegradable polylactide by solvent casting. Suyatma *et al.*[23] blended CS with PLA by solution mixing, and they found that the tensile strength of PLA blend increased from 52.5 ± 5.9 to 72.7 ± 1.8 MPa. However, the elongation at break of the CS/PLA blend was not significantly improved, and CS was immiscible with PLA.

It is important to note that fiber-reinforced composites are strongly influenced by the interactions of the components. The use of nanometer-sized fillers is able to increase the filler/PLA interface and reduce the loading content of the filler. When the active surface area of the particles is increased, the reaction rate and interface interaction increase.[23] The blending of biodegradable plastics with chitosan nanoparticles (CSNPs) have also been investigated. For example, Moura *et al.*[24] blended hydroxypropyl methylcellulose edible films with different particle size CS/tripolyphosphate nanoparticles. When the particle sizes of CS/tripolyphosphate nanoparticles were reduced from 221 to 85 nm, the tensile strength of the blended films increased from 38 to 63 MPa. They also found that the CS/tripolyphosphate nanoparticles (85 nm) enhanced the degradation temperature (T_d) of hydroxypropyl methylcellulose by 47°C. Chang *et al.*[25] improved glycerol-plasticized potato starch composites by blending with different contents of CSNPs. By increasing the CSNP content, the tensile strength of glycerol-plasticized potato starch/CSNP composites increased. On the basis of the literature, CS/PLA or CSNP/polymers blends were studied. To our knowledge, a strategy to modify colloidal CS with a compatibilizer as a biobased nanofiller for PLA blends has not yet been reported. Moreover, modification of CS with radiation-induced graft copolymerization has not also been yet demonstrated. It is known that radiation synthesis is an easy process and provides good efficiency and a noncatalyst in a reaction system.[26] With a very small object of ionizing radiations, that is, γ rays and electron beams, they have been considered a potential tool for the construction of nanostructural materials. CSNPs and their derivatives have been successfully prepared with γ irradiation.[26] In addition, a radiation-induced grafting technique can be carried out without an initiator and without a heating system. This technique is also able to be performed in a heterogeneous reaction because of the high penetration of the ionizing radiation.

The goal of this study was to modify CS with poly(ethylene glycol) methyl ether methacrylate (PEGMA) with radiation-induced graft copolymerization. The modified CSNPs were carefully characterized. The effects of the dose rate, irradiation dose, and PEGMA concentration on the degree of grafting (DG), particle formulation, and size were studied. The compatibility and thermal properties of the resulting CSNP/PLA blends were also investigated in this study.

EXPERIMENTAL

Materials

CS, with a degree of deacetylation of 95 [viscosity-average molecular weight (M_v) = 700 kDa], was supplied from Seafresh Chitosan (Lab) Co., Ltd. (Thailand). PEGMA (molecular weight = 950) was purchased from Sigma Aldrich. The PLA polymer (type 2002D, melt flow index = 4–8 g/10 min and specific gravity = 1.24 g/cm^3), with a weight-average molecular weight of about 150 kDa, was purchased from NatureWorks. Sodium hydroxide was obtained from Carlo Erba Reagent (Italy). Glacial acetic acid was purchased from Labscan Co., Ltd. (Thailand).

Instruments and Equipment

M_v of the CS raw material was measured with a standard method for dilute solution viscosity according to Pasanphan *et al.*[27] Briefly, the calibrated viscometer was used to determine M_v. A solvent mixture of 0.2*M* CH_3COOH and 0.1*M* CH_3COONa was prepared as a solvent system for M_v determination. M_v was calculated from the Mark–Houwink equation:

$$[\eta] = KM_v^a$$

where the constant values of K and a are 7.21×10^{-4} and 1.004, respectively, and $[\eta]$ is the intrinsic viscosity calculated from the experimental plot. M_v was determined according to a standard method (ASTM D 445). A Gammacell 220 irradiator and a Gamma irradiator (Mark I) was used as γ-rays sources for high and low dose rates of 4.7 and 0.78 kGy/h, respectively. A red-dyed poly(methyl methacrylate) dosimeter type Red 4304 was supplied from Harwell Dosimeter, Ltd. All of the samples were irradiated in air under ambient temperature and pressure. The measurement accuracy was ±10%. Such accuracy is, nevertheless, sufficient for most radiation-processing applications.[28] Fourier transform infrared (FTIR) spectra were collected with a Bruker Tensor 27 in attenuated total reflection mode with 32 scans at a 2-cm^{-1} resolution in a frequency range of 4000–600 cm^{-1}. X-ray diffraction (XRD) patterns were recorded by a Bruker AXS D8 Advance (Bruker, Germany). Thermal stability was analyzed in a Pyris 7 PerkinElmer thermogravimetric analysis (TGA) instrument at a heating rate of 10°C/min. The particle morphology and size were observed with a Hitachi H7650 Zero A transmission electron microscope (Japan). The morphology of the PLA blends in cross section was observed with a Quanta 450 FEI scanning electron microscope and a Hitachi SU8020 field emission scanning electron microscope (FE-SEM). A twin-screw extruder (Labtech Engineering) and a Battenfeld BA250 injection-molding machine were used for the blending

process. The tensile strength, elongation at break, and Young's modulus were determined with a universal testing machine (QC-506B, Cometech) with a load cell of 5 kN according to ASTM D 638 at room temperature.

Modification of CS with PEGMA by γ Irradiation

CS colloids in distilled water were prepared according to Pasanphan *et al.*[27] Briefly, CS (0.50% w/v) was predissolved with acetic acid (1% v/v). The solidified CS was precipitated in an aqueous sodium hydroxide solution (1% w/v) to obtain white colloids. The precipitated colloidal product was washed with water several times. The obtained CS colloids were kept by dispersed in distilled water. A series of PEGMA aqueous solutions (7.29% w/v for 0.30, 0.40, 1.20, 1.98, and 3.00 mL) were mixed with CS colloids (0.50% w/v, 15 mL). The samples were γ-irradiated with doses of 1, 2, 3, 5, 15, 25, and 40 kGy for a high dose rate of 4.7 kGy/h. The irradiation was carried out in an air atmosphere. The irradiated products were washed thoroughly with distilled water several times. The products were freeze-dried to a constant weight to obtain PEGMA-*graft*-CS nanoparticles (PEGMA-*graft*-CSNPs). The DG of PEGMA-*graft*-CSNPs was determined as follows:

$$[(W_G - W_0)/W_0] \times 100$$

where W_G and W_0 are the weights of the graft copolymer and starting CS, respectively. Similarly, studies on a low-dose-rate of 0.78 kGy/h with ^{137}Cs Gamma irradiator (Mark I) were also carried out with absorbed doses of 1, 2, and 3 kGy with the same procedure.

Compatibility and Thermal Stability of the PEGMA-*graft*-CSNP Blended PLA

PLA pellets were dried at 60°C in a vacuum oven, and the PEGMA-*graft*-CSNP powder was kept overnight in a desiccator before processing. The 2 and 4% w/w PEGMA-*graft*-CSNPs (70 ± 8 nm, 145% DG) were blended with PLA at 160–170°C with an applied laboratory hot press and compression mold with a temperature controller and rapidly cooled down in a water bath obtain a sheet with the thickness of 1 mm. The blended sheets were in liquid N_2 to observe the compatibility in cross section using SEM and FE-SEM. The thermal properties of the blended sheet were also measured with TGA.

Blending Process of PEGMA-*graft*-CSNP/PLA

PLA pellets were dried at 60°C in a vacuum oven, and the representative PEGMA-*graft*-CSNP powder (70 ± 8 nm, DG = 145%) synthesized at a high dose rate with the irradiation dose of 25 kGy was kept overnight in a desiccator before use. The mixture of PLA pellets and 2% w/w PEGMA-*graft*-CSNPs were prepared with a twin-screw extruder with a screw rotation speed of 22–24 rpm at 160–190°C and dried in air. The PEGMA-*graft*-CSNP/PLA blends were processed with an injection-molding machine with a screw diameter of 22 mm at 160°C according to ASTM D 638.

Mechanical Properties of the PEGMA-*graft*-CSNP Blended PLA

The tensile test was conducted according to ASTM D 638 at a crosshead speed of 5 mm/min with a universal testing machine with a load cell of 5 kN. The sample thickness was about 4 mm. The tensile mechanical properties include the tensile strength, elongation at break, and Young's modulus. An average of five individual determinations was obtained.

RESULTS AND DISCUSSION

A simultaneous grafting reaction was carried out in a heterogeneous system consisting of CS colloids in the PEGMA aqueous solution. Through radiation exposure of an aqueous medium in an air atmosphere, water radiolysis species are initially produced as shown in eq. (1). The hydroxyl radical ($HO^{\bullet}$) and hydrogen atom ($H^{\bullet}$) are themselves chemically reactive.[29,30] The $HO^{\bullet}$ and $H^{\bullet}$ basically abstract H atoms from the CS backbone; this leads to the creation of reactive sites on the polysaccharide chain of CS ($CS^{\bullet}$), as shown in eq. (2). The $CS^{\bullet}$ added to double bonds of the PEGMA monomer and led to the creation of a graft-growing chain, as shown in eq. (3) and Scheme 1(A). It is important to note that $CS^{\bullet}$ radicals were produced throughout CS colloids because of the high penetration of the γ radiation. However, under a heterogeneous reaction, we supposed that the PEGMA molecules mainly grafted onto the CS colloidal surface, adhering the PEGMA molecules in the grafting solution [Scheme 1(B)]. In the presence of oxygen, peroxyl radicals [CS—$OO^{\bullet}$; eq. (3)], hydroperoxide [CS—OOH; eq. (4)], and alkoxyl radical [CS—$O^{\bullet}$; eq. (5)] possibly took place. In this system, CS—$O^{\bullet}$ underwent an addition reaction to the double bond of PEGMA; this gave an ether bond linkage in the graft copolymer [eq. (7)] and underwent the following termination sequence [eqs. (8) and (9)].

Water radiolysis

$$H_2O \rightarrow e_{aq}^{-}, H^{\bullet}, HO^{\bullet}, H_2, H_2O_2, O_2^{-\bullet} \quad (1)$$

Graft copolymerization

$$CS{-}H + HO^{\bullet}(\text{or } H^{\bullet}) \rightarrow CS^{\bullet} + H_2O(H_2) \quad (2)$$

$$CS^{\bullet} + m\text{PEGMA} \rightarrow CS{-}\text{PEGMA}^{\bullet}{}_m \quad (3)$$

$$CS^{\bullet} + O_2 \rightarrow CS{-}OO^{\bullet} \quad (4)$$

$$CS{-}OO^{\bullet} + H^{\bullet} \rightarrow CS{-}OOH \quad (5)$$

$$CS{-}OOH \rightarrow CS{-}O^{\bullet} + HO^{\bullet} \quad (6)$$

$$CS{-}O^{\bullet} + m\text{PEGMA} \rightarrow CS{-}O{-}\text{PEGMA}^{\bullet}{}_m \quad (7)$$

$$CS{-}O{-}\text{PEGMA}^{\bullet}{}_m + H^{\bullet} \rightarrow CS{-}O{-}\text{PEGMA}_m{-}H \quad (8)$$

$$CS{-}O{-}\text{PEGMA}^{\bullet}{}_m + \text{PEGMA}^{\bullet}{}_n \rightarrow CS{-}O{-}\text{PEGMA}_{m+n} \quad (9)$$

Homopolymerization

$$HO^{\bullet} + \text{PEGMA} \rightarrow HO{-}\text{PEGMA}^{\bullet} \quad (10)$$

$$HO{-}\text{PEGMA}^{\bullet} + n\text{PEGMA} \rightarrow HO{-}\text{PEGMA}^{\bullet}{}_{n+1} \quad (11)$$

$$HO{-}\text{PEGMA}^{\bullet}{}_{n+1} + H^{\bullet} \rightarrow HO{-}\text{PEGMA}_{n+1}{-}H \quad (12)$$

Chain scission of CS

$$CS^{\bullet}(\text{or } CS{-}O^{\bullet}) \rightarrow CS_1 + CS_2\text{fragments} \quad (13)$$

In addition to grafting, the chain scission of CS and the homopolymerization of PEGMA possibly occurred. The radiation-induced chain scission of CS generally takes place at 1–4 glycosidic linkage. Radiolysis and radiation-induced degradation of CS have been reported in previous articles.[29,30] However, in this grafting reaction, the graft copolymerization might have

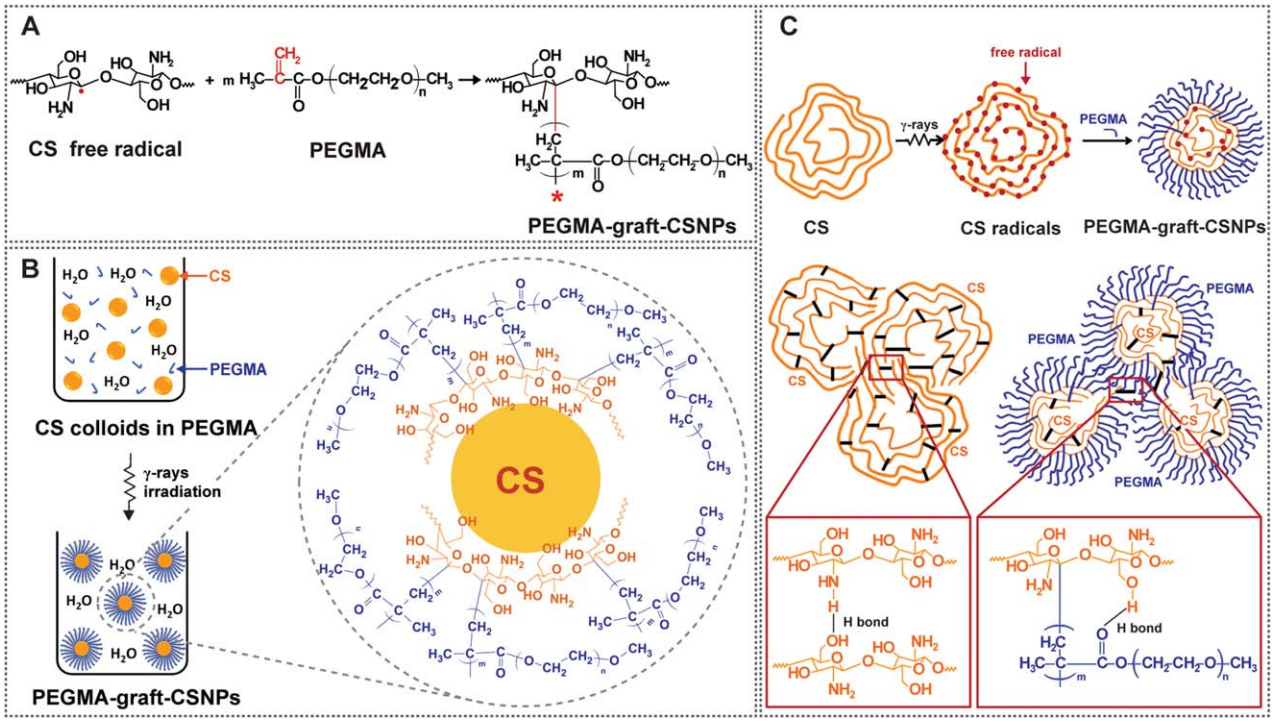

Scheme 1. (A) Mechanism, (B) synthesis route, and (C) interaction of PEGMA-*graft*-CSNPs from radiation-induced graft copolymerization. [Color figure can be viewed in the online issue, which is available at wileyonlinelibrary.com.]

predominated because of the presence of the reactive vinyl terminal group of the PEGMA monomer. Because of the simultaneous radiation-induced grafting system, homopolymerization possibly occurred, as shown in eqs. (10–12). Therefore, the poly[poly (ethylene glycol) methyl ether methacrylate] [poly(-PEGMA)] homopolymer was carefully removed by washing with distilled water several times. It has been reported that poly(PEGMA) was soluble in water.[31] Basically, PEG and its derivatives are poly(ether diol)s containing two terminal hydroxyl groups (—OH) and many alternating ether (C—O—C) linkages. Thus, PEGs have a lot of diol character, and they are more soluble in water. For PEG with higher molecular weights, it has more polyether character, and the solubility is due to hydrogen bonding. The solubility in water could be explained by the hydrogen bonding of the water molecules to the electron-rich oxygen atoms in the PEG or PEGMA polymer chain.[32]

Chemical Structure of PEGMA-*graft*-CSNPs Observed by FTIR Spectroscopy

The characteristic peaks of CS, PEGMA, and PEGMA-*graft*-CS with different DGs could be identified by FTIR spectroscopy. Figure 1(A-a) shows the characteristic peaks of CS at 896 cm^{-1} (pyranose ring), 1652 cm^{-1} (amide I), 1593 cm^{-1} (amide II), and 3353 cm^{-1} (O—H stretching overlapping with N—H stretching).[33] For PEGMA [Figure 1(A-b)], the major peaks at 2888, 1719, 1630, 843–960, and 1103 cm^{-1} belonging to C—H stretching, carbonyl groups (C═O), double bonds (C═C), and ether bonds (C—O—C) were observed. Proof of the successful preparation of the PEGMA-*graft*-CSNPs was extracted from the FTIR spectra, as shown in Figure 1(A-c–e). The representative FTIR spectra of the PEGMA-*graft*-CSNPs prepared from different conditions are displayed in Figure 1(A-c,d). The FTIR spectrum of the PEGMA-*graft*-CSNPS produced from a high dose rate and low dose of 3 kGy [Figure 1(A-c)] was equivalent to the FTIR spectrum of CS [Figure 1(A-a)]. The result suggests that PEGMA moieties could not be grafted onto CS. Thus, the DG of this sample was equal to zero. Figure 1(A-d,e) shows disappearance of the FTIR peaks around 843–960 cm^{-1} associated with the double bonds in the PEGMA structure. This implied the successful radical polymerization of PEGMA. Compared to FTIR spectrum of CS [Figure 1(A-a)], a new peak around 1727 or 1724 cm^{-1} clearly appeared for PEGMA-*graft*-CSNPs, as shown in Figure 1(A-d,e)]. This peak was interpreted as the carbonyl group (C═O) of the grafted PEGMA. In contrast to the PEGMA spectrum [Figure 1(A-b)], the carbonyl peaks of PEGMA-*graft*-CSNPs [Figure 1(A-d,e)] were shifted from 1716 to 1727 or 1724 cm^{-1} as a result of successful grafting. The FTIR result is relevant to previous research.[26] The functional groups observed from the FTIR spectra confirmed that the PEGMA moieties were successfully decorated onto CS by radiation-induced grafting.

Packing Structure of the PEGMA-*graft*-CSNPs Observed by XRD

The confirmation of the grafted materials was described through the packing structure observed by XRD. Typical XRD patterns of the CS and PEGMA-*graft*-CSNPs from different DGs are shown in Figure 1(B). The neat CS exhibited three prominent peaks at 2θs of 10.2, 19.8, and 21.9° with a broad diffraction because of its amorphous to partially crystalline state

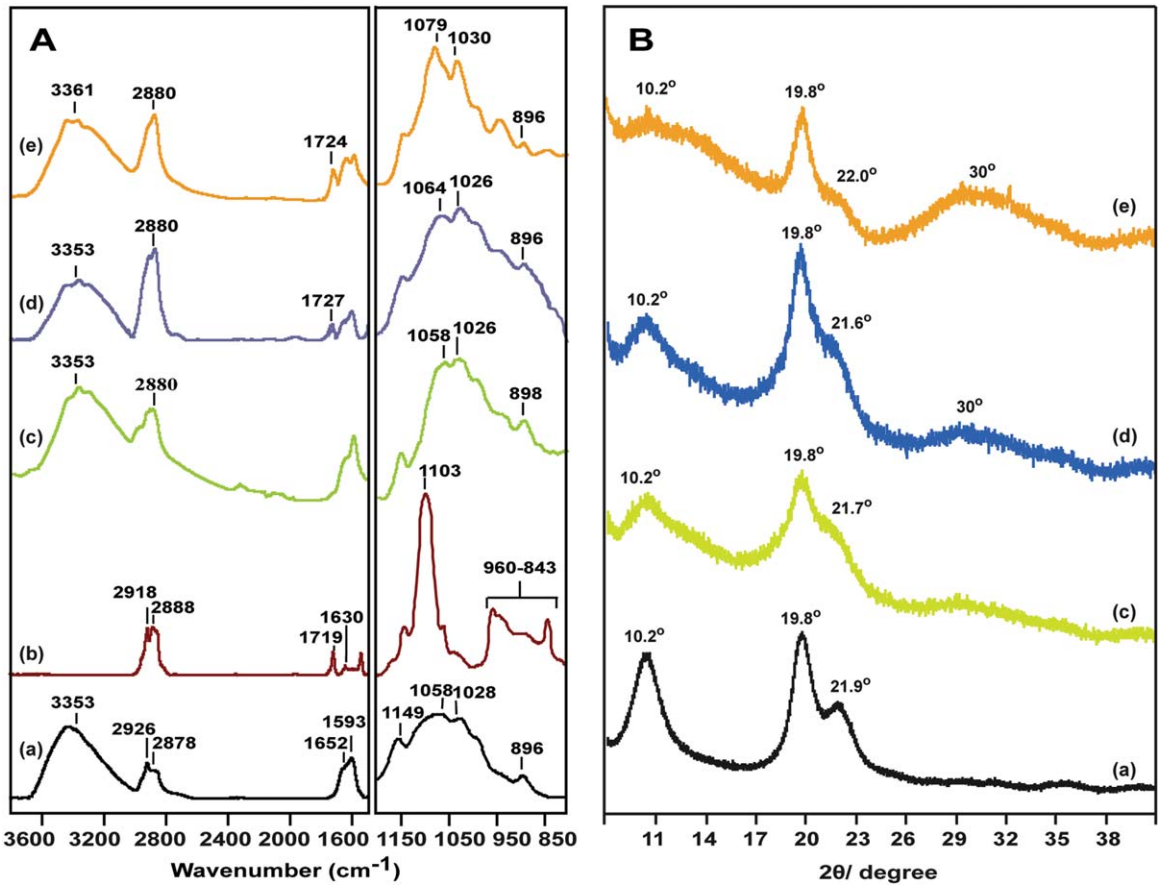

Figure 1. (A) FTIR spectra and (B) XRD patterns of (a) CS, (b) PEGMA, (c) PEGMA-*graft*-CSNPs (DG = 0%) synthesized at 3 kGy (high dose rate), (d) PEGMA-*graft*-CSNPs (DG = 26%) synthesized at 25 kGy (high dose rate), and (e) PEGMA-*graft*-CSNPs (DG = 57%) synthesized at 3 kGy (low dose rate). [Color figure can be viewed in the online issue, which is available at wileyonlinelibrary.com.]

[Figure 1(B-a)]. This observation was in accordance with many previous studies. A peak at a 2θ of approximately 10.2° corresponded to hydrated crystals, and the one around a 2θ of 19.8° belonged to anhydrous crystals because of the intermolecular and intramolecular hydrogen bonding of CS.[34–36] After radiation-induced grafting [Figure 1(B-b–d)], the basic diffraction peaks were maintained, but some peak intensities changed considerably, and a new peak evidently appeared. For the PEGMA-*graft*-CSNP sample with a DG of 0% [Figure 1(B-b)], the XRD pattern seemed to be identical with the neat CS; this confirmed that there was no grafted PEGMA. A somewhat broaden spectrum might be a slight decrease in the crystalline portion as a result of a radiation effect. The insignificant change of the XRD pattern in Figure 1(B-b) confirmed that the PEGMA could not be effectively grafted onto CS with an inadequate dose only of 3 kGy under high-dose-rate conditions. This was in agreement with the unchanged FTIR spectrum shown in Figure 1(A-c). With increasing DG [Figure 1(B-c,d)], the diffraction peak at a 2θ of 10.2° became broad, particularly at a higher DG of 57%. Its presence could be explained as a result of the grafted PEGMA moieties, which barred the intermolecular hydrogen bonding of CS. In addition, a slight increase in the peak at 19.8° and the presence of a new peak at a 2θ of 30° of the PEGMA-*graft*-CSNPs may have been due to the characteristic crystalline structure of the grafted poly(-PEGMA).[37] It has been previously denoted that the PEGMA moieties were mainly grafted onto the CS surface because of the heterogeneous reaction [Scheme 1(C)]. However, the XRD pattern of PEGMA-*graft*-CSNPs was measured in the dried formulation. Thus, the PEGMA grafted on CS hindered the packing structure of each CS particle.[38] Compared with the PEGMA-*graft*-CSNPs, the nongrafted CS commonly packed each other because of its hydrogen bonds [Scheme 1(C)]. A comparison of the XRD profiles indicated that the grafted PEGMA on CS partially destroyed the original crystallinity of CS. These changes in the diffraction patterns suggested that the difference in the packing structure of the chains and/or the difference of the hydrogen-bonding network in the copolymer.[39,40] The changes in the packing structure observed by XRD confirmed that the PEGMA moieties were engaged with CS.

Thermal Stability of the PEGMA-*graft*-CSNPs Observed by TGA

The weight loss curve of the CS and PEGMA-*graft*-CSNPs with two different DGs under heating in an oxygen atmosphere are shown in Figure 2. For the first weight loss stage (50–100°C),

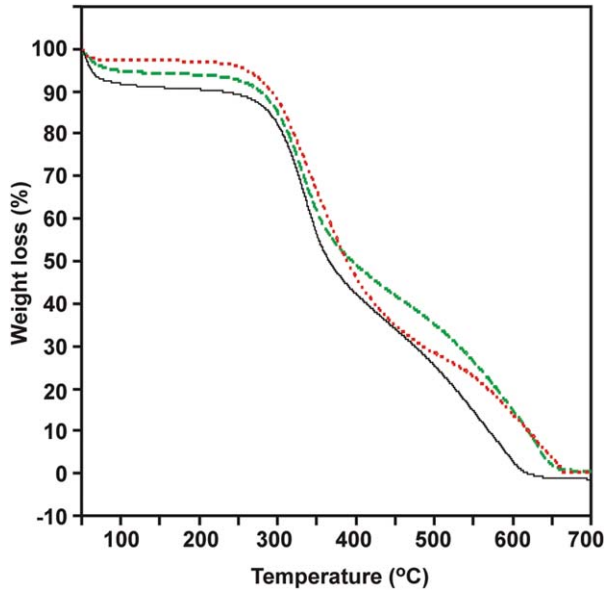

Figure 2. TGA curves of (—) CS, (· · ·) PEGMA-*graft*-CSNPs (DG = 145%) synthesized at 25 kGy (high dose rate), and (- - -) PEGMA-*graft*-CSNPs (DG = 57%) synthesized at 3 kGy (low dose rate). [Color figure can be viewed in the online issue, which is available at wileyonlinelibrary.com.]

the CS and PEGMA-*graft*-CSNPs with DG of 57 and 145% decomposed with weight losses of 10, 6, and 3%, respectively. These weight losses indicated the decomposition of the absorbed and bound water, including small volatile molecules.[41] Both the CS and PEGMA-*graft*-CSNPs showed two significant stages of weight loss. After the first decomposition, the CS started to decompose at an onset temperature of 306°C and reached a maximum at 376°C with a weight loss of 33%, and it completely decomposed to about 32% until 614°C. Compared with CS, the PEGMA-*graft*-CSNPs with a DG of 57% showed a higher second stage of weight loss of 35% spanning from 275 to 357°C and another weight loss of 35%, with continuous decomposition until 650°C. With increasing DG up to 145%, the weight loss increased to 54% within the temperature range of 280–426°C, and it continued to decompose for 23% until 662°C. These decompositions were interpreted as the weight losses of the CS and grafted poly(PEGMA). An increase in the weight loss of CS in the second stage of decomposition could be described from the grafted PEGMA moieties; this obstructed the hydrogen bonds and partially destroyed the crystalline structure of CS [Scheme 1(C)].[42] The results are in agreement with the packing conformation observed by XRD.

We also found that the T_d values of the CS and PEGMA-*graft*-CSNPs with DGs of 57 and 145% were 342, 321, and 336°C, respectively. The increase of T_d with increasing DG implied a higher thermal stability because of the higher amount of grafted poly(PEGMA). The results demonstrate that the PEGMA-*graft*-CSNPs with a higher DG of 145% exhibited more thermal stability than that with a lower DG of 57%. We suspected that the new hydrogen bond between the graft poly(PEGMA) and CS might have also formed [Scheme 1(C)]; this resulted in an increase of the thermal stability in the case of a high DG of

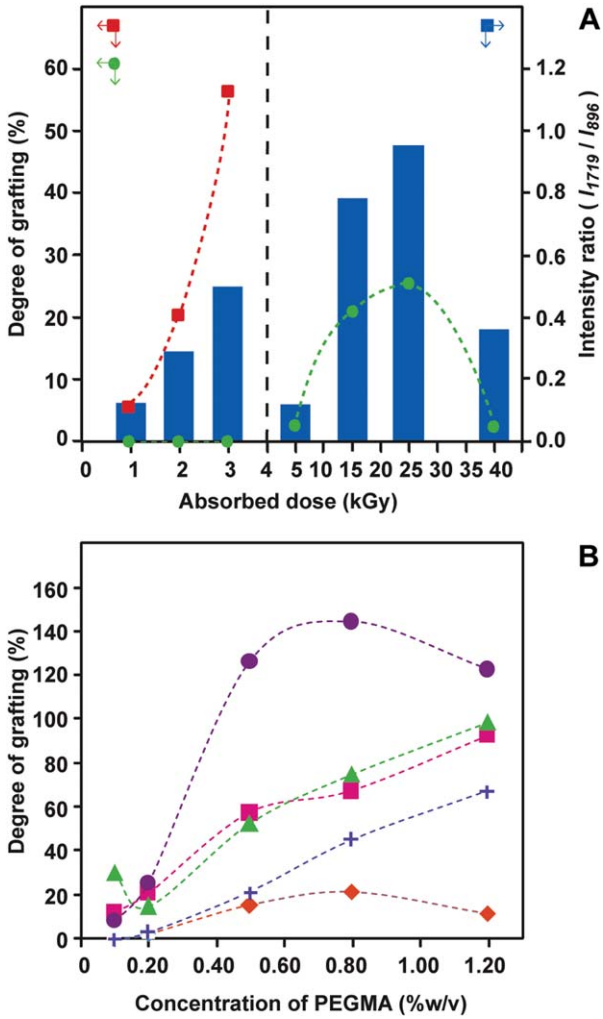

Figure 3. (A) Effects of low dose rates (orange squares) and high dose rates (green circles) on the DG and FTIR intensity ratios [histogram (blue square)]. (B) Effect of the PEGMA concentration on the DG of PEGMA-*graft*-CSNPs prepared with high dose rates: 5 (orange diamonds), 15 (pink squares), 20 (green triangles), 25 (purple circles), and 40 kGy (blue crosses). [Color figure can be viewed in the online issue, which is available at wileyonlinelibrary.com.]

145%. As additional proof, the remarkable difference in the thermal properties between the CS and PEGMA-*graft*-CSNPs with different DGs illustrated that the PEGMA moieties were successfully grafted onto CS.

Effects of Dose Rate and Irradiation Dose on DG

In the radiation-induced graft copolymerization system, the dose rate is one of the parameters that affects the grafting efficacy.[43] Figure 3(A) shows the DG of PEGMA onto CS and the applied doses at two different dose rates, 0.78 and 4.7 kGy/h. The concentration of PEGMA in the initial grafting mixture was 0.2% w/v in an aqueous solution. DG increased with irradiation dose for these two different dose rates. Compared with the high dose rate, the low dose rate resulted in a significant increase in DG from 5 to 57% when the dose increased from 1 to 3 kGy. On the other hand, DG at a high dose rate was not observed when the samples were irradiated under a dose range of 1–3

kGy. We reported that at a high dose rate, the radicals forming on the CS colloid tended to decay by radical combination faster than at a lower dose rate.[44] This phenomenon subsequently resulted in a lower availability of radical sites on the polymer substrate for the grafting reaction. At a higher dose rate, the PEGMA growing radical was also created more quickly and consequently propagated and terminated by recombination; this resulted in a high homopolymer and gave a lower DG. It is also important to note that at a higher dose rate, the grafted poly(PEGMA) chains were subjected to faster termination and/or degradation, and subsequently, the DG decreased. The results observed in this study were in agreement with other works, in which styrene was grafted onto poly(tetrafluoroethylene-*co*-perfluoropropylvinyl ether)[44,45] and poly(ethylene terephthalate)[46] with γ irradiation under simultaneous system.

DG evidently increased from 2 to 26% when the irradiation dose was increased from 5 to 25 kGy (right panel). The increase in DG with an increase of dose was basically due to higher amount of free radicals in the grafting system.[47,48] However, after the irradiation dose increased excessively up to 40 kGy, the DG declined to less than 5%. It is known that in a simultaneous system, the PEGMA monomer not only added to the radical on the graft-growing chain [CS—O—PEGMA$^{\bullet}_{m}$; eq. (7)] but also polymerized to form the PEGMA homopolymer [HO—PEGMA$^{\bullet}_{n+1}$; eq. (10)]. These continuously happened when the irradiation time was prolonged because of the increase of the irradiation dose. Therefore, the grafting solution became viscous because of the grafted shell and the homopolymer. Accordingly, the monomers migrated difficultly to the reactive site of the grafted chain and the DG reduction sequence.[49] With an excessive irradiation dose as high as 40 kGy, the radiation-induced degradation of the previously grafted PEGMA chain possibly took place and DG tended to decrease.

To ensure the relationship between the irradiation doses and DG, the relative FTIR intensity ratios were determined. The amount of grafted PEGMA could be estimated by the amount of the ester bond in the PEGMA structure presented in the PEGMA-graft-CSNPs product. Therefore, the increase of the ester bond peak intensity at 1719 cm^{-1} (I1719) in comparison with the pyranose ring peak intensity at 896 cm^{-1} (I896) could confirm the amount of grafting. Hence, the FTIR intensity ratio of I1719/I896 was determined. It was found that the intensity ratios were in agreement with the DG along with the irradiation doses.

Effects of the PEGMA Concentration and Irradiation Dose on DG

To examine the effects of the PEGMA concentration and irradiation dose on the grafting amount, the DG values were plotted against the PEGMA concentrations, as presented in Figure 3(B). We found that DG increased with increasing PEGMA concentration. At a low irradiation dose of 5 kGy, DG increased slightly to 20% with increasing PEGMA concentration to 0.80%. With moderate irradiation doses of 15 and 20 kGy, DG increased steadily with similar values along with increasing PEGMA concentrations from 0.10 to 1.20%. The irradiation doses of 15 and 20 kGy brought about insignificant different grafting efficacies. For 25 kGy, DG increased to a maximum value of 145% at 0.08% PEGMA. However, DG tended to level off when the concentration reached 1.20%. At a high monomer concentration, the PEGMA monomer became closer, and homopolymerization took place easily. The homopolymerization of PEGMA gave a more viscous grafting solution. This might obstruct the diffusion of the PEGMA monomer and/or its radical to the grafted growing chain on the CS substrate.[48] If this occurred, the homopolymerization would take place over graft copolymerization, giving a lower DG.

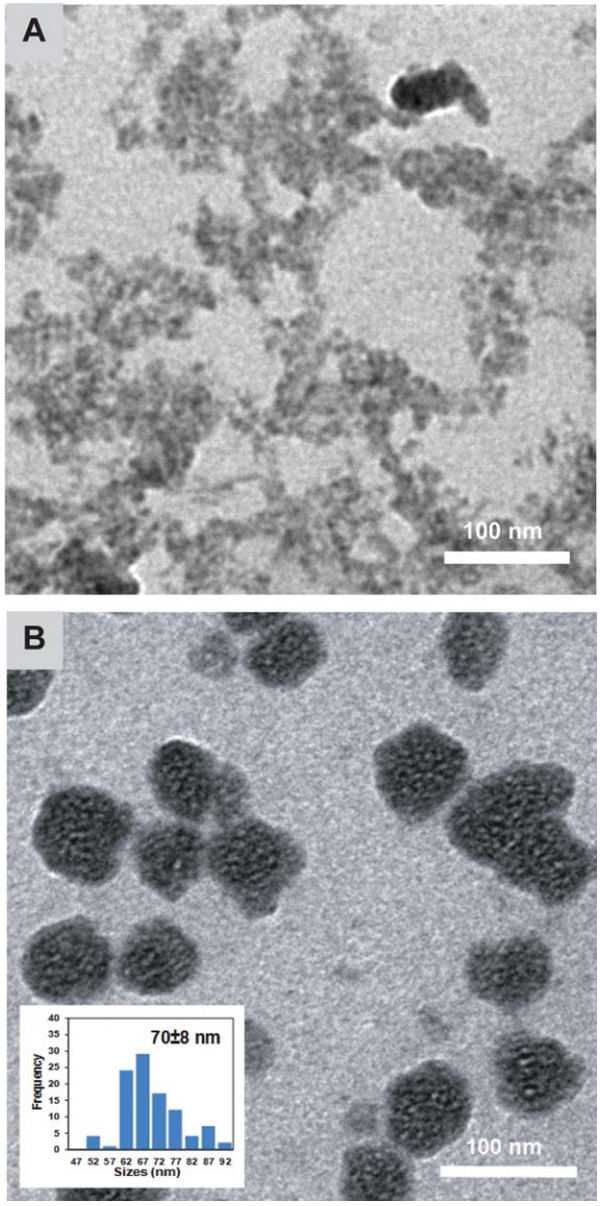

Figure 4. TEM images and size distribution plot (inset) of (A) CS colloids and (B) PEGMA-*graft*-CSNPs (DG = 145%). [Color figure can be viewed in the online issue, which is available at wileyonlinelibrary.com.]

Particle Morphology and Size of the PEGMA-*graft*-CSNPs Observed by the TEM

The morphologies of the CS colloids and the representative PEGMA-*graft*-CSNPs (145%DG) are shown in Figure 4(A,B), respectively. As shown in the TEM image, the CS colloids

Table I. DGs and Particle Sizes of the PEGMA-*graft*-CSNPs Synthesized under Different Conditions

Condition	Dose rate (kGy/h)	Dose (kGy)	[PEGMA] (w/v %)	DG (%)	Particle size (nm)
Low dose rate	0.78	1	0.20	5	86 ± 6
		2	0.20	20	92 ± 5
		3	0.20	57	104 ± 7
High dose rate	4.7	25	0.20	26	35 ± 4
		25	0.80	145	70 ± 8

exhibited aggregation with a nonuniform structure. Compared with CS, the particle morphology of the PEGMA-*graft*-CSNPs revealed individually self-assembled particles with a nanoscopic spherical shape [Figure 4(B)]. The average particle size was randomly determined from the representative TEM images. The particle size of the PEGMA-*graft*-CSNPs was 70±8 nm with a very narrow size distribution. It is know that CS cannot be dissolved in water; on the other hand, the CS modified with the *m*PEGs derivative was possible because of the degree of substitution of *m*PEGs on CS. It has also been reported that *m*PEGs-*graft*-CS spontaneously formed nanometer-sized aggregates through strong intermolecular hydrogen bonds between the CS moieties.[50] Halabalová and Šimek[51] also reported that dipole–dipole or hydrogen bonding should be responsible for the interaction between CS and PEG in the solution. Therefore, favorable interactions could have occurred between amide or amine nitrogen on the CS backbone and the hydroxyl and etheric oxygen of the PEG. In this study, the grafted poly(-PEGMA) contained several carbonyl groups (C═O) in the methacrylate structure and the ethylene oxide group (—CH_2—CH_2—O—) in the repeating unit of PEGMA [Scheme 1(C)]. Thus, hydrogen bonding could randomly take place between both groups in the poly(PEGMA) and —OH or —NH_2 groups on the CS chains.[52] We demonstrated that the interactions between CS and PEGMA reflected the particle morphology of the PEGMA-*graft*-CSNPs.

The effect of DG on the particle sizes of the PEGMA-*graft*-CSNPs was observed and is shown in Table I. We found that the average particle size was larger with increasing DG. For a low dose rate, the particle size increased from 86 ± 6 to 92 ± 5 and 104 ± 7 nm when DG increased from 5 to 20 and 57%, respectively. Similarly, at a high dose rate, the particle size increased from 35 ± 4 to 70 ± 8 nm with increasing DG from 26 to 145%. In comparison with the low dose rate, the PEGMA-*graft*-CSNPs prepared from a high dose rate had a significant smaller particle size, even though their DGs were mostly identical (20 and 26%). We assumed that the dose used for grafting also affect the particle size of the resulting PEGMA-*graft*-CSNPs. As shown in Table I, the PEGMA-*graft*-CSNPs (26%DG) from the high dose rate was synthesized with a higher irradiation dose of 25 kGy, whereas the PEGMA-*graft*-CSNPs (20%DG) from the low dose rate could only be prepared with 2 kGy. In addition to radiation-induced grafting, we also suspected that radiation-induced degradation of the CS main chain occurred upon simultaneous grafting reaction [eq. (13)].[28] This was also another parameter affecting the particle size of the resulting PEGMA-*graft*-CSNPs.

Compatibility of the PEGMA-*graft*-CSNP/PLA Blends

Because improved PEG is generally used as a plasticizer study, we aimed to modify CS with PEGMA to prepare a novel compatible biobased nanofiller for the PLA blends. Clarification of the compatibility between the PEGMA-*graft*-CSNPs and PLA is important. SEM was used to confirm the miscibility of the blends, as shown in Figure 5(A). The neat PLA showed a clear morphology [Figure 5(A-a)]. PLA blended with 2% w/w CS [Figure 5(A-b)] evidently showed phase separation between PLA and nonmodified CS, whereas PLA blended with 2% w/w PEGMA-*graft*-CSNPs (DG = 145%, 70 ± 8 nm) showed compatibility with the PLA matrix [Figure 5(A-c)].

To confirm the compatibility of the nanoscaled PEGMA-*graft*-CSNPs, including nonmodified CS in the PLA matrix, FESEM was also carried out, and the images are shown in Figure 5(B). It is known that FESEM is capable of measuring high-quality imaging solutions in nanostructural morphology. The representative FESEM images of the neat PLA, PLA with 2% w/w CS, and PEGMA-*graft*-CSNPs are revealed in Figure 5(B-a–c). The neat PLA showed a clear morphology, as observed with SEM, whereas PLA with 2% w/w CS [Figure 5(B-b)] exhibited a significant phase separation between the nonmodified CS and PLA matrix. This evidently confirmed the incompatibility of CS in the PLA matrix. The low interaction between these two components was an underlying reason. In comparison to neat PLA, the PLA blended with 2% w/w of PEGMA-*graft*-CSNPs [DG = 145%, 70 ± 8 nm; Figure 5(B-c)] showed a smooth and homogeneous morphology in cross section. We gathered that the grafting of PEGMA onto CS was able to improve the compatibility between CS and PLA. The compatibility observed by FESEM strongly confirmed the successful production of the PEGMA-*graft*-CSNPs as the compatible biobased nanofiller for PLA.

Thermal Stability of the PEGMA-*graft*-CSNP/PLA Blends

To observe the effect of the PEGMA-*graft*-CSNPs in the PLA matrix on the thermal properties, TGA was carried out to investigate the weight loss profile and T_d. Figure 6 displays the TGA results of the neat PLA and PLA blended with the PEGMA-*graft*-CSNPs with different loading contents of 2 and 4% w/w. The neat PLA degraded in a single stage within a narrow temperature ranging from 364 to 403°C with a T_d of 394°C, in agreement with literature reports.[54,55] Compared to the neat PLA, the onset decomposition temperature of the PLA

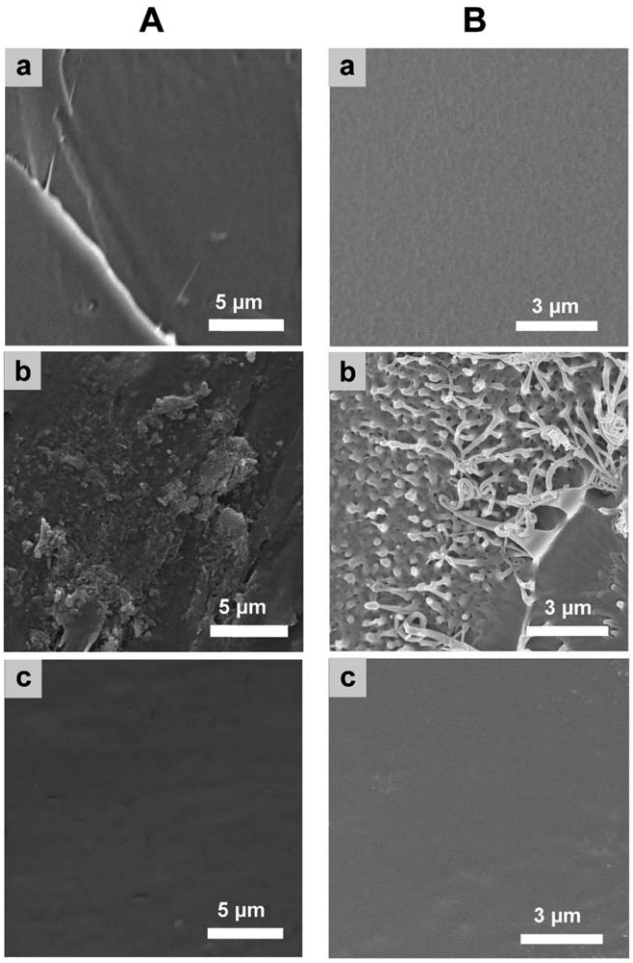

Figure 5. (A) SEM and (B) FESEM images of (a) neat PLA, (b) PLA blended with 2% (w/w) CS, and (c) PLA blended with 2% w/w PEGMA-*graft*-CSNPs (DG = 145%). [Color figure can be viewed in the online issue, which is available at wileyonlinelibrary.com.]

containing 2 and 4% w/w PEGMA-*graft*-CSNPs increased from 394 to 396 and 408°C, respectively. The results show that the thermal stability significantly increased by 14°C at a very low loading content of 4% w/w. The PEGMA-*graft*-CSNP/PLA blend possessed a higher thermal stability compared to the neat PLA; this was due to the high thermal stability of CS. The better adhesion between the PEGMA-*graft*-CSNPs and PLA matrix (Figure 5) may help to reduce the diffusion of volatile decomposition products as a result of the homogeneous dispersion of the PEGMA-*graft*-CSNPs within the polymer blend.[56] The thermal stability of the PEGMA-*graft*-CSNP/PLA blend was comparable to PLA containing modified montmorillonite (3% w/w); the thermal stability increased with 10–15°C.[54] Al-Mulla *et al.*[57] also reported that T_d of PLA increased by 14% when fatty acid/montmorillonite (3% w/w) was added in the epoxidized oil plasticized PLA. The use of PEGMA-*graft*-CSNPs improved not only the compatibility but also the thermal stability of PLA, whereas the use of a small-molecular-weight PEG plasticizer promoted a decrease in the thermal stability by breaking the polymer–polymer interaction.[58] Although more detail about the

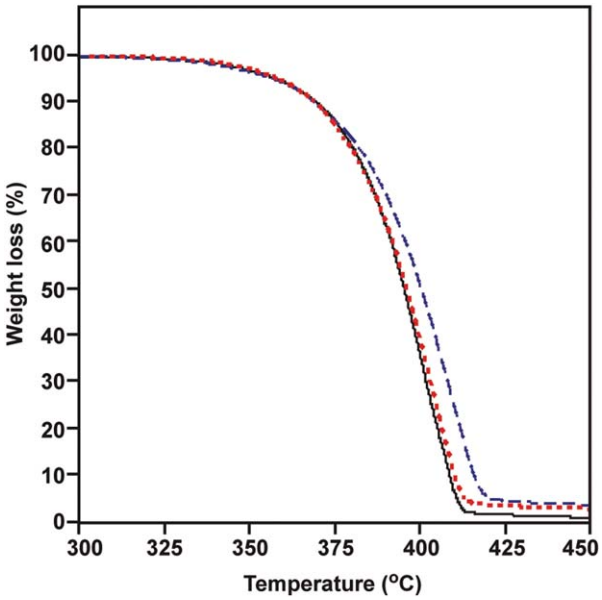

Figure 6. TGA curves of (—) neat PLA and PLA blended with (· · ·) 2 and (- - -) 4% w/w PEGMA-*graft*-CSNPs (DG = 145%). [Color figure can be viewed in the online issue, which is available at wileyonlinelibrary.com.]

PEGMA-*graft*-CSNP/PLA blend performance is needed, from our preliminary data compared to the other fillers, the PEGMA-*graft*-CSNPs would be considerable as a novel biobased nanofiller for PLA blends.

Mechanical Properties of the PEGMA-*graft*-CSNP/PLA Blends

To observe how the PEGMA-*graft*-CSNPs affected the mechanical properties of the PLA blends, the tensile stress–elongation curves of PLA and its blends with CS and PEGMA-*graft*-CSNPs were

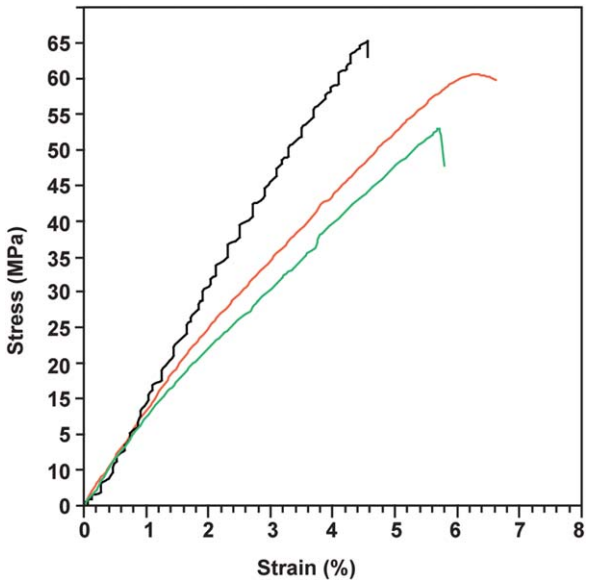

Figure 7. Stress–strain curves of the neat PLA (black line), PLA blended with 2% w/w CS (green line), and PLA blended with 2% w/w PEGMA-*graft*-CSNPs (DG = 145%, 70 ± 8 nm; orange line). [Color figure can be viewed in the online issue, which is available at wileyonlinelibrary.com.]

Table II. Tensile Mechanical Properties of the Neat PLA and PLA Blended with CS and PEGMA-*graft*-CSNPs

Sample	Tensile strength (MPa)	Elongation at break (%)	Young's modulus (MPa)
PLA	64.8 ± 0.9	4.56 ± 0.20	1639 ± 324
CS/PLA (2% w/w)	52.9 ± 2.3	5.72 ± 0.81	918 ± 340
PEGMA-*graft*-CS/PLA (2% w/w)	60.8 ± 0.6	6.12 ± 0.97	1183 ± 208

measured, as shown in Figure 7. Compared to the neat PLA, CS/PLA, and PEGMA-*graft*-CSNP/PLA blends exhibited more extension. The most prominent feature was that the PEGMA-*graft*-CSNP/PLA blend showed some necking behavior and ductile features. This is known as a mode of tensile deformation or the amount of plasticity before fraction. The greater ductility is, the more a material can be deformed. Therefore, the PEGMA-*graft*-CSNP/PLA blend displayed somewhat ductile characteristics, whereas the neat PLA and CS/PLA blend were still brittle.

The tensile mechanical properties are summarized in Table II. The tensile strength was about 64.8 MPa for the neat PLA, and it decreased to 52.9 and 60.8 MPa for PLA blended with 2% w/w CS and PEGMA-*graft*-CSNPs, respectively. There was an 18.36% decrease in the tensile strength when the nonmodified CS was blended with PLA. This was attributable to the poor dispersion of CS in the PLA matrix, as discussed previously (Figure 5). We reported that the effect of incompatibility on the mechanical properties of the composites was substantial.[59] Although the tensile strength of the PEGMA-*graft*-CSNPS/PLA blend showed a slight decrease of 6.17% when compared with the neat PLA, the PEGMA-*graft*-CSNP/PLA blend had a greater tensile strength than the nonmodified CS. This illustrated the behavior of grafted PEGMA to improve the compatibility between the two phases.

It is known that PLA is a rigid and brittle polymer with a very low elongation at break. The material breaks after yield without necking, as indicated in the stress–strain curve (Figure 7). The elongations at break of the neat PLA and the CS/PLA and PEGMA-*graft*-CSNP/PLA blends were 4.56, 5.72, and 6.12%, respectively. The elongations at break of CS/PLA and PEGMA-*graft*-CSNP/PLA blends increased by 25.44 and 34.21%, respectively, compared with that of the neat PLA.

The brittleness of the samples was observed from the tensile modulus results. Compared with that of the neat PLA, the tensile modulus of the CS/PLA and PEGMA-*graft*-CSNP/PLA blends decreased by 43.99 and 27.82%, respectively. The results suggest that CS showed a tendency to reduce the rigid properties of the PLA. However, the CS/PLA blend still broke after yield without necking as a result of brittleness. The PEGMA-*graft*-CSNP/PLA blend exhibited more flexibility when compared with PLA and more ductility when compared with PLA and CS/PLA. The results suggest that the flexibility improvement was due to the CS segment, and the ductility improvement was due to the grafted PEGMA brush segment.[58] The elongation at break and modulus results demonstrate that the PEGMA-*graft*-CSNPs not only improved the compatibility between CS and PLA but also improved the ductility and flexibility of the PLA.

CONCLUSIONS

A novel biobased compatible nanofiller was successfully synthesized by grafting PEGMA onto CS using radiation-induced graft copolymerization technique. The particle sizes of PEGMA-*graft*-CSNPs were ranging from 30–100 nm; this depended on DG and the synthesis parameters, that is, the dose rate, dose, and PEGMA concentration. The DGs of PEGMA on CS were 3–145%. On the basis of the preliminary studies on the compatibility of the PEGMA-*graft*-CSNP/PLA blends, the PEGMA-*graft*-CSNPs significantly improved the compatibility between CS and PLA. With a low loading content of 4% w/w, the thermal stability of PEGMA-*graft*-CSNP/PLA increased by 14°C. The mechanical characteristics of the PEGMA-*graft*-CSNP/PLA blends showed an increase of the percent elongation at break and a decrease of the tensile modulus. This means that the transition of PLA characteristics from brittle to more ductile behavior. We will extend our work in the future to study the performance of the mechanical properties of the PEGMA-*graft*-CSNP/PLA blends.

ACKNOWLEDGMENTS

The authors acknowledge the Kasetsart University Research and Development Institute, the National Research Council of Thailand, and the budget for Overseas Academic Conference (Faculty of Science, Kasetsart University) for their financial support. They gratefully thank the Office of Atom for Peace (Ministry of Science and Technology, Thailand) and the Gamma Irradiation Service and Nuclear Technology Research Center (Kasetsart University) for γ-irradiation services. Appreciation is also expressed to Suwabun Chirachanchai (Petroleum and Petrochemical College, Chulalongkorn University, Thailand) for the TEM measurements.

REFERENCES

1. Tokiwa, Y.; Calabia, B. P.; Ugwu, C. U.; Aiba, S. *Int. J. Mol. Sci.* **2009**, *10*, 3722.
2. Yu, L.; Dean, K.; Li, L. *Prog. Polym. Sci.* **2006**, *31*, 576.
3. Ogata, N.; Jimenez, G.; Kawai, H.; Ogihara, T. *J. Polym. Sci. Part B: Polym. Phys.* **1997**, *35*, 389.
4. Rasal, R. M.; Janorkar, A. V.; Hirt, D. E. *Prog. Polym. Sci.* **2010**, *35*, 338.
5. Takatani, M.; Ikeda, K.; Sakamoto, K.; Okamoto, T. *J. Wood. Sci.* **2008**, *54*, 54.
6. Chabrat, E.; Abdillahi, E.; Rouilly, A.; Rigal, L. *Ind. Crop Prod.* **2012**, *37*, 238.
7. Kangwanwatthanasiri, P.; Suppakarn, N.; Ruksakulpiwat, C.; Ruksakulpiwat, Y. *Adv. Mater. Res.* **2013**, *747*, 367.

8. Sheth, M.; Kumar, R. A.; Dave, V.; Gross, R. A.; McCarthy, S. P. *J. Appl. Polym. Sci.* **1997**, *66*, 1495.
9. Sinclair, R. G. *J. Macromol. Sci. Chem.* **1996**, *33*, 585.
10. Ulasan, M.; Yavuz, E.; Bagriacik, E. U.; Cengeloglu, Y.; Yavuz, M. S. *J. Biomed. Mater. Res. A* **2015**, *103*, 243.
11. Favaro Ferrarezi, M. M.; Oliveira Taipina, M.; Escobar da Silva, L. C.; Goncalves, M. C. *J. Polym. Environ.* **2013**, *21*, 151.
12. Chieng, B. W.; Ibrahim, N. A.; Wan Yunus, W. M. Z.; Hussein, M. Z. *J. Appl. Polym. Sci.* **2013**, *130*, 4576.
13. Park, B. S.; Song, J. C.; Park, D. H.; Yoon, K. B. *J. Appl. Polym. Sci.* **2012**, *123*, 2360.
14. Alcantar, N. A.; Aydil, E. S.; Israelachvili, J. N. *J. Biomed. Mater. Res.* **2000**, *51*, 343.
15. Jacobsen, S.; Fritz, H. G. *Polym. Eng. Sci.* **1999**, *39*, 1303.
16. Choudhary, P.; Mohanty, S.; Nayak, S. K.; Unnikrishnan, L. *J. Appl. Polym. Sci.* **2010**, *121*, 3223.
17. Yuan, Y.; Ruckenstein, E. *Polym. Bull.* **1998**, *40*, 485.
18. Lu, D. R.; Xiao, C. M.; Xu, S. *J. Express Polym. Lett.* **2009**, *3*, 366.
19. Shah, B. L.; Selke, S. E.; Walters, M. B.; Heiden, P. A. *Polym. Compos.* **2008**, *29*, 655.
20. Qu, P.; Gao, Y.; Wu, G. F.; Zhang, L. P. *Bioresources* **2010**, *5*, 1811.
21. Correlo, V. M.; Boesel, L. F.; Bhattacharya, M.; Mano, J. F.; Neves, N. M.; Reis, R. L. *Mater. Sci. Eng. A.* **2005**, *403*, 57.
22. Wan, Y.; Wu, H.; Yu, A.; Wen, D. *Biomacromolecules* **2006**, *7*, 1362.
23. Suyatma, N. E.; Copinet, A.; Tighzert, L.; Coma, V. *J. Polym. Environ.* **2004**, *12*, 1.
24. Moura, M. R.; Aouada, F. A.; Avena-Bustillos, R. J.; McHugh, T. H.; Krochta, J. M.; Mattoso, L. H. C. *J. Food Eng.* **2009**, *92*, 448.
25. Chang, P. R.; Jian, R.; Yu, J.; Ma, X. *Food Chem.* **2010**, *120*, 736.
26. Pasanphan, W.; Rattanawongwiboon, T.; Rimdusit, P.; Piroonpan, T. *Radiat. Phys. Chem.* **2014**, *94*, 199.
27. Pasanphan, W.; Rimdusit, P.; Choofong, S.; Piroonpan, T.; Nilsuwankosit, S. *Radiat. Phys. Chem.* **2010**, *79*, 1095.
28. Fernandez, F. A.; Brichard, B.; Ooms, H.; Nieuwenhove, R. W.; Berghmans, F. *Nucl. Sci.* **2005**, *52*, 505.
29. Ulanski, P.; Rosiak, J. *Int. J. Radiat. Appl. Instrum. Radiat. Phys. Chem.* **1992**, *39*, 53.
30. Hai, L.; Diep, T. B.; Nagasawa, N.; Yoshii, F.; Kume, T. *Nucl. Instrum. Methods Phys. Res. Sect. B* **2003**, *208*, 466.
31. Miao, J.; He, W.; Zhang, L.; Wang, Y.; Cheng, Z.; Zhu, X. *J. Polym. Sci. Part A: Polym. Chem.* **2012**, *50*, 2194.
32. Brownstein, A. In the Chemistry of Polyethylene Glycol, Proceedings of the ICOM Waterlogged Wood Working Group Conference, Ottawa, Sept, 15–18, 1981, Grattan, D., Ed.; ICOM Waterlogged Wood Working Group: Ottawa, **1982**.
33. Fangkangwanwong, J.; Yoksan, R.; Chirachanchai, S. *Polymer* **2006**, *47*, 6438.
34. Burkhanova, N. D.; Yuai, S. M.; Pulatova, K. P.; Nikonovich, G. V.; Milusheva, R. Y.; Voropaeva, N. L.; Rashidova, S. S. *Chem. Nat. Compd.* **2000**, *36*, 352.
35. Nunthanid, J.; Puttipipatkhachorn, S.; Yamamoto, K.; Peck, G. E. *Drug Dev. Ind. Pharm.* **2001**, *27*, 143.
36. Pasanphan, W.; Buettner, G. R.; Chirachanchai, S. *J. Appl. Polym. Sci.* **2008**, *109*, 38.
37. Papadimitriou, S. A.; Achilias, D. S.; Bikiaris, D. N. *Int. J. Pharm.* **2012**, *430*, 318.
38. Deng, L.; Qi, H.; Yao, C.; Feng, M.; Dong, A. *J. Biomater. Sci. Polym. Ed.* **2007**, *18*, 1575.
39. Luckachan, G. E.; Pillai, C. K. S. *Carbohydr. Polym.* **2006**, *64*, 254.
40. Deng, L.; Qi, H.; Yao, C.; Feng, M.; Dong, A. *J. Biomater. Sci. Polym. Ed.* **2007**, *18*, 1575.
41. Spinelli, V. A.; Laranjeira, M. C. M.; Favere, V. T. *React. Funct. Polym.* **2004**, *61*, 347.
42. Zhou, G.; Ma, C.; Zhang, G. *Polym. Chem.* **2011**, *2*, 1409.
43. Dessouki, A. M.; El-Tahawy, M.; El-Boohy, H.; El-Mongy, S. A.; Badawy, S. M. *Radiat. Phys. Chem.* **1999**, *54*, 627.
44. Cardona, F.; George, G. A.; Hill, D. J. T.; Rasoul, F.; Maeji, J. *Macromolecules* **2002**, *35*, 355.
45. Nasef, M. M.; Saidi, H.; Nor, H. M.; Dahlan, K. Z. M.; Hashim, K. J. *Appl. Polym. Sci.* **1999**, *73*, 2095.
46. Nasef, M. M. *J. Appl. Polym. Sci.* **1999**, *77*, 1003.
47. Chapiro, A. Radiation Chemistry of Polymeric Systems; Wiley: New York, **1962**.
48. Nasef, M. M.; Hegazy, E. S. A. *Prog. Polym. Sci.* **2004**, *29*, 499.
49. Nizam El-Din, H. M. M.; Badawy, S. M.; Dessouki, A. M. *J. Appl. Polym. Sci.* **2000**, *77*, 1405.
50. Deng, L.; Qi, H.; Yao, C.; Feng, M.; Dong, A. *J. Biomater. Sci. Polym. Ed.* **2007**, *18*, 1575.
51. Halabalová, V.; Šimek, L. *Int. J. Polym. Anal. Char.* **2006**, *11*, 185.
52. Avérous, L.; Pollet, E. Biodegradable Polymers; Springer: London, **2012**; Chapter 2.
53. Ferrarezi, M. M. F.; Oliveira Taipina, M.; Silva, L. C. E.; Goncalves, M. C. *J. Polym. Environ.* **2013**, *21*, 151.
54. Fukushima, K.; Murariu, M.; Camino, G.; Dubois, P. *Polym. Degrad. Stab.* **2010**, *95*, 1063.
55. Hassouna, F.; Raquez, J. M.; Addiego, F.; Dubois, P.; Toniazzo, V.; Ruch, D. *Eur. Polym. J.* **2011**, *47*, 2134.
56. Abdolmohammadi, S.; Siyamak, S.; Ibrahim, N. A.; Wan Yunus, W. M. Z.; Rahman, M. Z. A.; Azizi, S.; Fatehi, A. *Int. J. Mol. Sci.* **2012**, *13*, 4508.
57. Al-Mulla, E. A. J.; Suhail, A. H.; Aowda, S. A. *Ind. Crop Prod.* **2011**, *33*, 23.
58. Chieng, B. W.; Ibrahim, N. A.; Wan Yunus, W. M. Z.; Hussein, M. Z. *Appl. Polym. Sci.* **2013**, *130*, 4576.
59. Wu, C. S. *Polym. Adv. Technol.* **2012**, *23*, 463.